AIAA JOURNAL
Vol. 35, No. 5, May 1997

Instability of Lightly Damped Linear Nonconservative Systems

Yeong-Bin Yang*
National Taiwan University, Taipei, Taiwan 10617, Republic of China
Shyh-Rong Kuo†
National Taiwan Ocean University, Keelung, Taiwan 20224, Republic of China
and
Jong-Dar Yau‡
National Taiwan University, Taipei, Taiwan 10617, Republic of China

In computing the critical load for a linear nonconservative system, one needs to construct the load-frequency curve from the characteristic equation that contains asymmetric matrices, based on the finite element formulation. Traditionally, this requires repeated solution of complex eigenvalues from the characteristic equation at many load levels, which is extremely time consuming in practice. Small damping of the Rayleigh type is assumed. A bieigenvalue curve is adopted to approximate the load-frequency curve for the first few modes of interest. Such a curve can be uniquely determined, once the derivatives of the frequency with respect to the load parameter have been calculated for a preset load level. After the bieigenvalue curve is established, the critical load can be computed by setting its first derivative equal to zero. The effectiveness of the present method is demonstrated in the numerical study.

Introduction

THE instability of nonconservative structures has been a subject of intensive research for many decades. In the literature, both linear[1–6] and nonlinear[7,8] systems have been studied. The objective of this paper is to formulate an efficient method for computing the critical loads of lightly damped linear nonconservative systems. To this end, the finite element formulation will be adopted for its versatility in modeling structures of various complexities. No attempt will be made to deal with the instabilities of nonlinear nonconservative systems.

With the finite element method, the nonconservative nature of applied loads is considered through an asymmetric load matrix. To compute the critical load for the nonconservative system, first, one has to construct the load-frequency curve from the characteristic equation. Traditional approaches aimed at establishing such a curve require repeated solution of complex eigenvalues from the characteristic equation, which is extremely time consuming in practice, as the original system has to be augmented into one with twice the number of degrees of freedom (DOFs). To improve the efficiency of solution, a bisection method based on the eigenvalue sensitivity has been proposed in Ref. 9. Unfortunately, this method can only deal with problems of the flutter type, for which two different frequencies become coincident, but not problems of the divergence type, for which one frequency reduces to zero.

In this paper, the damping of the structure is assumed to be small and of the Rayleigh type. By the method of perturbation and by neglecting terms of orders higher than two, the characteristic equation for the structure can be transformed into one identical in form to that for the undamped nonconservative structures. The critical load for the latter can then be computed through use of an approximate load-frequency curve for relating the first few modes that are of interest. Such a curve, referred to as the bieigenvalue curve,[10] can be uniquely determined once the first and second derivatives of the frequency with respect to the load parameter are calculated for a preset load level. With the present approach, it can be demonstrated that even for the case with no iteration, i.e., based on the eigensolutions obtained from free vibration analysis, critical loads of rather good accuracy can still be obtained and that for all of the problems considered, only three iterations are required to achieve convergent results. Because the complex characteristic equations need only be solved for a limited number of load levels, the efficiency of the present method is guaranteed. This study can be regarded as an extension of previous work on undamped nonconservative systems.[10]

Received June 4, 1996; revision received Feb. 7, 1997; accepted for publication Feb. 7, 1997.

*Professor and Chairman, Department of Civil Engineering.
†Associate Professor, Department of Harbor and River Engineering.
‡Postdoctoral Researcher, Department of Civil Engineering.

Asymmetric Load Matrix

Two typical configurations will be identified for a structure. One is the prebuckling configuration C_1 and the other is the buckled configuration C_2. As shown in Fig. 1, the space frame element consisting of 12 DOFs has been expressed in the stationary coordinates of C_1. To describe the path-dependent nature of a follower force acting at the element nodes, another set of coordinates $\alpha\beta\gamma$ fixed on the cross section of each node has to be introduced (Fig. 2).

Consider, for instance, a follower force of magnitude $(F_\alpha, F_\beta, F_\gamma)$ acting at node A of the element (Fig. 2), which can be expressed in the C_1 coordinates as

$$\{{}^1F\}^T = \{{}^1F_x \quad {}^1F_y \quad {}^1F_z\} \tag{1}$$

Let $\{u\}$ denote the displacement of node A from C_1 to C_2,

$$\{u\}^T = \{\{d\}^T \quad \{\theta\}^T\} \tag{2}$$

It consists of three translations and three rotations,

$$\{d\}^T = \{u \quad v \quad w\} \tag{3a}$$

$$\{\theta\}^T = \{\theta_x \quad \theta_y \quad \theta_z\} \tag{3b}$$

For the case of small rotations, the transformation matrix $[T]$ that relates the axes $\alpha\beta\gamma$ at the C_1 configuration to the C_2 configuration is

$$[T] = \begin{bmatrix} 1 & \theta_z & -\theta_y \\ -\theta_z & 1 & \theta_x \\ \theta_y & -\theta_x & 1 \end{bmatrix} \tag{4}$$

Hence, the follower force $(F_\alpha, F_\beta, F_\gamma)$ at the buckled configuration C_2 can be expressed in the C_1 coordinates as

$$\{{}^2F\} = [T]\{{}^1F\} = \{{}^1F\} + \{\Delta F\} = \{{}^1F\} + [k_f]\{\theta\} \tag{5}$$

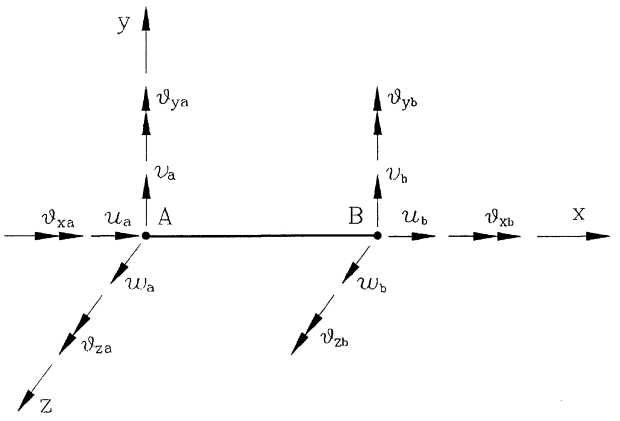

Fig. 1 Space frame element.

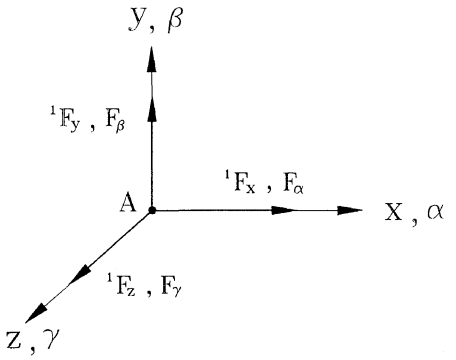

a) C_1 configuration

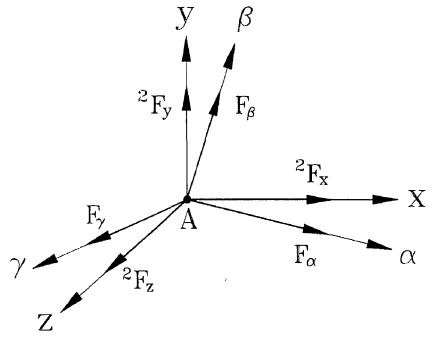

b) C_2 configuration

Fig. 2 Follower forces.

where the last term represents the forces induced by the follower force undergoing rotations. The load matrix $[k_f]$ is

$$[k_f] = \begin{bmatrix} 0 & {}^1F_z & -{}^1F_y \\ -{}^1F_z & 0 & {}^1F_x \\ {}^1F_y & -{}^1F_x & 0 \end{bmatrix} \tag{6}$$

which appears to be skew symmetric.

By defining the virtual works done by the follower force, respectively, at C_1 and C_2 for node A of the element as

$$^1\delta W = \{\delta d\}^T\{^1F\} \tag{7a}$$

$$^2\delta W = \{\delta d\}^T\{^2F\} = \{\delta d\}^T\{^1F\} + \{\delta d\}^T[k_f]\{\theta\} \tag{7b}$$

the virtual work done by the induced forces in the buckling stage can be computed:

$$^2\delta W - {}^1\delta W = \{\delta d\}^T[k_f]\{\theta\} = \{\delta u\}^T[k_l]\{u\} \tag{8}$$

where the displacement vector $\{u\}$ has been defined in Eq. (2) for node A of the element (Fig. 1) and the load matrix $[k_l]$ can be augmented from $[k_f]$ as

$$[k_l] = \begin{bmatrix} [0] & [k_f] \\ [0] & [0] \end{bmatrix} \tag{9}$$

Though the foregoing derivation has been made only for node A, it can be extended in a straightforward manner to node B of the element.

Linearized Theory of Stability

With the load matrix $[k_l]$ just derived and the elastic stiffness matrix $[k_e]$, geometric stiffness matrix $[k_g]$, and mass matrix $[m]$ available elsewhere,[11–13] the equation of motion can be written for each element. Using the element equations, the equation of motion for the structure can be assembled in incremental form as

$$[M]\{\ddot{U}\}+[C]\{\dot{U}\}+([K_e]+[K_g]-[K_l])\{U\} = \{^2P\}-\{^1P\} \tag{10}$$

where all terms have been expressed in the C_1 coordinates, the uppercase letters denote quantities associated with the structure, $\{^1P\}$ and $\{^2P\}$ are the applied loads acting on the structure at C_1 and C_2, respectively, and $\{U\}$ are the buckling displacements generated during the step from C_1 to C_2. In particular, the load matrix $[K_l]$ contains terms only for those nodes where the follower loads are applied. The geometric stiffness matrix $[K_g]$ should be assembled with the rotational properties of joint moments taken into account.[12,13] Based on the assumption of Rayleigh damping, the matrix $[C]$ can be calculated as

$$[C] = a_1[K_e] + a_2[M] \tag{11}$$

where a_1 and a_2 denote the internal and external damping coefficients, respectively.

When in buckling, the applied loads acting on the structure remain constant, i.e., $\{^2P\} = \{^1P\} = \{P\} = \lambda\{\bar{P}\}$, where $\{\bar{P}\}$ denotes a reference load vector and λ the associated load parameter. For the case of small prebuckling deformations, both the $[M]$ and $[K_e]$ matrices can be regarded as constant and the $[K_g]$ and $[K_l]$ matrices as proportional to the applied loads. Accordingly, Eq. (10) reduces to

$$[M]\{\ddot{U}\} + [C]\{\dot{U}\} + ([K_e] + \lambda[\bar{K}_g] - \lambda[\bar{K}_l])\{U\} = \{0\} \tag{12}$$

where $[\bar{K}_g]$ and $[\bar{K}_l]$ denote the matrices evaluated for the structure under the action of the reference loads $\{\bar{P}\}$ prior to buckling.

Based on the assumption of small damping, the matrix $[C]$ given in Eq. (11) can be rewritten as

$$[C] = \epsilon\{[K_e] + \beta[M]\}, \qquad \epsilon \ll 1 \tag{13}$$

where β denotes the ratio of the external to internal damping, i.e., the external damping ratio. By letting ω denote the frequency of vibration of the structure under the action of constant loads, the displacements of the structure can be denoted as $\{U\} = \{\bar{U}\}e^{i\omega t}$. Substituting this expression for $\{U\}$ and Eq. (13) for $[C]$ into Eq. (12) yields

$$\big(-\omega^2[M] + i\epsilon\omega([K_e] + \beta[M]) + [K_e] + \lambda([\bar{K}_g] - [\bar{K}_l])\big)\{\bar{U}\} = \{0\} \tag{14}$$

where λ and ω^2 are the eigenpair and $\{\bar{U}\}$ the associated eigenvector.

Statement of the Problem

Let α_k^2 and $\{v_k\}$ denote the kth eigenvalue and eigenvector of a J-dimensional subset of the N-DOF structure that has zero damping and is free of any applied loads, i.e.,

$$\big(-\alpha_k^2[M] + [K_e]\big)\{v_k\} = \{0\} \tag{15}$$

where $k = 1, 2, \ldots, J$ and $J \leq N$. Moreover, let $[V]$ denote the modal matrix comprising only the first J eigenvectors, i.e.,

$[V] = [\{v_1\}, \ldots, \{v_J\}]$. The following properties of orthogonality are known to be valid:

$$[V]^T[M][V] = [I] \tag{16}$$

$$[V]^T[K_e][V] = [\Lambda] = \begin{bmatrix} \ddots & & 0 \\ & \alpha_k^2 & \\ 0 & & \ddots \end{bmatrix} \tag{17}$$

With these properties, Eq. (14) can be converted to the following:

$$\left(-\omega_k^2[I] + i\epsilon\omega_k(\beta[I] + [\Lambda]) + [\Lambda] + \lambda[A]\right)\{\phi_k\} = \{0\} \tag{18}$$

$$\{\Psi_k\}^T\left(-\omega_k^2[I] + i\epsilon_k(\beta[I] + [\Lambda]) + [\Lambda] + \lambda[A]\right) = \{0\}^T \tag{19}$$

where $\{\phi_k\}$ and $\{\psi_k\}$ are the right and left eigenvectors of the kth mode of the damped structure and

$$[A] = [V]^T([\bar{K}_g] - [\bar{K}_l])[V] \tag{20}$$

By letting $[\Phi] = [\{\phi_1\}, \ldots, \{\phi_J\}]$ and $[\Psi] = [\{\psi_1\}, \ldots, \{\phi_J\}]$, it can be shown that

$$[\Psi]^T[\Phi] = [I] \tag{21}$$

Before Eq. (18) or (19) can be solved, they have to be transformed into a system containing twice the number of DOFs of the original system. For instance, Eq. (18) can be transformed as follows:

$$-\omega_k\begin{pmatrix}[I] & [0] \\ [0] & [\Lambda] + \lambda[A]\end{pmatrix}\begin{pmatrix}\omega_k\{\phi_k\} \\ \{\phi_k\}\end{pmatrix} + \begin{pmatrix}i\epsilon\{[\lambda] + \beta[I]\} & [\Lambda] + \lambda[A] \\ [\Lambda] + \lambda[A] & [0]\end{pmatrix}\begin{pmatrix}\omega_k\{\phi_k\} \\ \{\phi_k\}\end{pmatrix} = \{0\} \tag{22}$$

It is not always easy to solve this equation even using modern commercial codes.

The stability of a structure under the action of load $\{\bar{P}\}$ can be observed from the property of the frequency of vibration ω solved from the characteristic equation, as given in Eq. (14) or (22). For instance, by letting $\omega = a + ib$, one can write

$$\{U\} = \{\bar{U}\}e^{iat} \cdot e^{-bt} \tag{23}$$

When the imaginary part of ω, i.e., the variable b, is negative, the displacements $\{U\}$ of the structure become unbounded. In this case, the structure is regarded as unstable within the framework of linear analysis.

Two types of instability can be identified from the characteristic equation of a nonconservative system.[10] One is the so-called divergence or static instability, which is characterized by the occurrence of a negative ω^2 when the load parameter λ exceeds the critical load λ_{cr} (see Fig. 3a). For this special case, the critical load λ_{cr} can be determined from the characteristic equation by setting $\omega^2 = 0$ through a single call to any eigenvalue solver that is capable of dealing with asymmetric systems.

The other is the so-called flutter or dynamic instability, which is typified by the occurrence of complex ω^2 when the load parameter λ exceeds the critical value λ_{cr} (see Fig. 3b). For the special case of $\lambda = \lambda_{cr}$, two eigenroots ω^2 become coincident. To compute the critical value λ_{cr}, one conventional approach is to divide the load $\{P\}$ into a number of increments, as shown in Fig. 4a, and then compute the eigenvalues ω^2 for each load level. By connecting all of the solved points (λ, ω^2) in the load-frequency plot, the critical value λ_{cr} can, thus, be determined. Obviously, if solutions of sufficient accuracy are desired, much smaller load increments should be used as the critical load λ_{cr} is approached (see Fig. 4a). One drawback with such an approach is that it requires repeated calls to the complex eigenvalue solver, which is cost prohibitive.

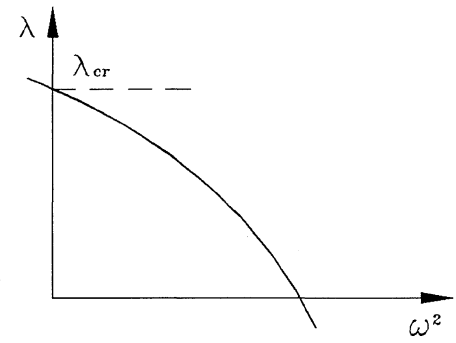

a) Divergence

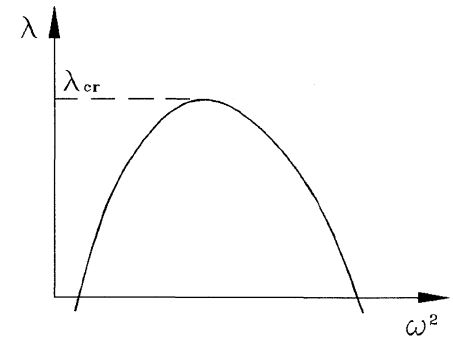

b) Flutter

Fig. 3 Types of instability.

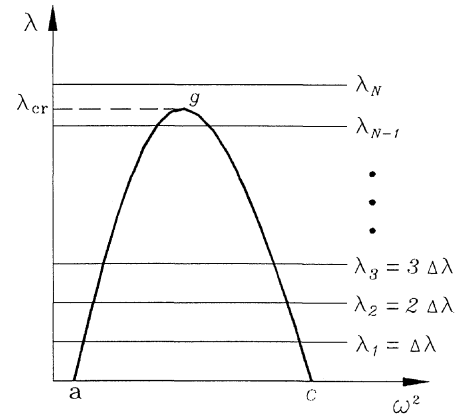

a) Conventional

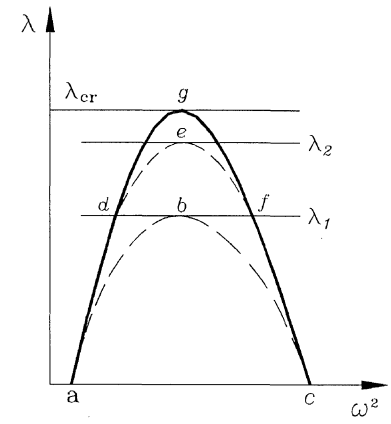

b) Present

Fig. 4 Methods of solution.

Method of Perturbation

In this section, the method of perturbation will be adopted to solve the critical loads λ_{cr} from the characteristic equation. Let

$$\{\phi_k\} = \{\phi_k\}_0 + \epsilon\{\phi_k\}_1 + \cdots = \sum_{n=0}^{\infty} \epsilon^n \{\phi_k\}_n \tag{24a}$$

$$\omega_k = (\omega_k)_0 + \epsilon(\omega_k)_1 + \cdots = \sum_{n=0}^{\infty} \epsilon^n (\omega_k)_n \tag{24b}$$

Substituting Eq. (24) into Eq. (18), expanding with respect to ϵ, and collecting all of the terms associated with ϵ^0, one obtains

$$\big(-(\omega_k)_0^2[I] + [\Lambda] + \lambda[A]\big)\{\phi_k\}_0 = \{0\} \tag{25}$$

A comparison of Eq. (25) with Eq. (18) indicates that the terms $(\omega_k)_0$ and $\{\phi_k\}_0$ in Eq. (25) represent the kth frequency and vibration vector (right eigenvector) of the structure with zero damping, i.e., with $\epsilon = 0$. Similarly, one may show that the following relations are satisfied by the left eigenvector $\{\psi_k\}_0$:

$$\{\psi_k\}_0^T\big(-(\omega_k)_0^2[I] + [\Lambda] + \lambda[A]\big) = \{0\}^T \tag{26}$$

$$\{\psi_k\}_0^T\{\psi_l\}_0 = \delta_{kl} \tag{27}$$

where δ is the Kronecker delta. From Eqs. (25–27), the following can be derived:

$$-(\omega_k)_0^2 + s_k^* + \lambda a_k^* = 0 \tag{28}$$

where

$$s_k^* = \{\psi_k\}_0^T[\Lambda]\{\phi_k\}_0 \tag{29a}$$

$$a_k^* = \{\psi_k\}_0^T[A]\{\phi_k\}_0 = \frac{\mathrm{d}(\omega_k)_0^2}{\mathrm{d}\lambda} \tag{29b}$$

To prove the relation $a_k^* = \mathrm{d}(\omega_k)_0^2/\mathrm{d}\lambda$ in Eq. (29b), let us differentiate Eq. (25) by λ:

$$\left(-\frac{\mathrm{d}(\omega_k)_0^2}{\mathrm{d}\lambda}[I] + [A]\right)\{\phi_k\}_0 + [B_k]\frac{\mathrm{d}}{\mathrm{d}\lambda}\{\phi_k\}_0 = \{0\} \tag{30}$$

where

$$[B_k] = -(\omega_k)_0^2[I] + [\Lambda] + \lambda[A] = [\Phi][D_k][\Psi]^T \tag{31}$$

$$[D_k] = \begin{bmatrix} \omega_1^2 - (\omega_k)_0^2 & & 0 \\ & \ddots & \\ 0 & & \omega_J^2 - (\omega_k)_0^2 \end{bmatrix} \tag{32}$$

By multiplying Eq. (30) by $\{\psi_k\}_0^T$ and using Eq. (26), the relation $a_k^* = \mathrm{d}(\omega_k)_0^2/\mathrm{d}\lambda$ can be proved. Thus, the term a_k^* should be interpreted as the first derivative of the frequency ω_0^2 with respect to the load parameter λ for the structure with zero damping.

Similarly, by collecting all of the terms associated with ϵ^1 in the series expansion, the following can be obtained:

$$\big(-(\omega_k)_0^2[I] + [\Lambda] + \lambda[A]\big)\{\phi_k\}_1$$

$$= \big(2(\omega_k)_0 \cdot (\omega_k)_1[I] - i(\omega_k)_0(\beta[I] + [\Lambda])\big)\{\phi_k\}_0 \tag{33}$$

Multiplying both sides of Eq. (33) by $\{\psi_k\}_0$ and using Eqs. (26) and (27), one can derive the following:

$$(\omega_k)_1 = (i/2)\big(\beta + s_k^*\big) \tag{34}$$

By neglecting all of the terms of orders higher than ϵ^2, the expression for ω_k in Eq. (24b) can be approximated as

$$\omega_k \approx (\omega_k)_0 + \epsilon(\omega_k)_1 \tag{35}$$

Based on the fact that internal damping tends to reduce the critical load of a nonconservative system,[1–3] one may conceive that the same system with zero damping should remain in the stable condition, for which the frequency $(\omega_k)_0$ is a real number. By substituting Eq. (34) into Eq. (35), the imaginary part of the frequency ω_k for the damped system can be obtained as

$$\mathrm{Im}(\omega_k) \approx (\epsilon/2)\big(\beta + s_k^*\big) \tag{36}$$

This equation can be used to judge the stability of a damped system. If the term $\mathrm{Im}(\omega_k)$ is less than zero, the system is considered unstable, as can be seen from Eq. (23).

Substituting s_k^* from Eq. (28) into Eq. (36), along with Eq. (29b) for a_k^*, yields

$$\mathrm{Im}(\omega_k) = \frac{\epsilon}{2}\left[\beta + (\omega_k)_0^2 - \lambda\frac{\mathrm{d}}{\mathrm{d}\lambda}(\omega_k)_0^2\right] \tag{37}$$

From the characteristic curve shown in Fig. 5a for a lightly damped structure, one observes that if the eigenpairs (λ, ω) are located in segment ab, then

$$\beta + (\omega_k)_0^2 - \lambda\frac{\mathrm{d}}{\mathrm{d}\lambda}(\omega_k)_0^2 > 0 \tag{38}$$

In Fig. 5a, point b refers to the point of the tangent connected from point o to the characteristic curve, and point o is determined by the external damping ratio β. As can be seen from Eq. (37), for a lightly damped structure with its eigenpairs (λ, ω) falling in the range ab, it remains in the stable state. On the other hand, for a structure with its eigenpairs located in the range bc, it is in a state of instability. Obviously, point b serves as the critical point for identifying the dynamic instability of a lightly damped structure. At this point, it is known that

$$\beta + (\omega_k)_0^2 = \lambda\frac{\mathrm{d}}{\mathrm{d}\lambda}(\omega_k)_0^2 \tag{39}$$

which is exactly the condition for detecting the dynamic instability of a lightly damped nonconservative structure.

From the series expansion of Eq. (18), it can be observed that the terms associated with ϵ^2 is a real number. By Eqs. (24b), (36), and (23), it can be seen that the influence of damping on the dynamic instability is determined by terms up to the order of ϵ^2. Thus, for nonconservative structures with small damping, the critical load can be accurately predicted using Eq. (39).

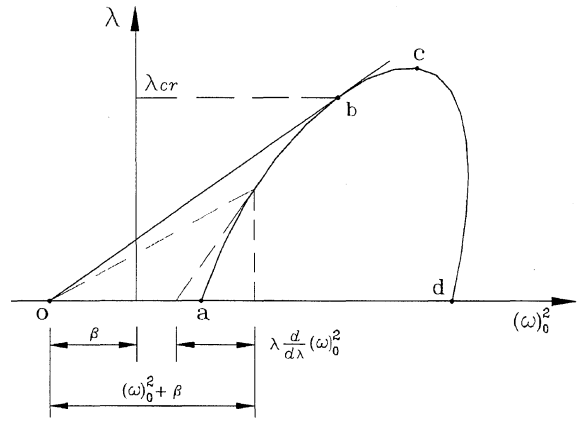

a) Original

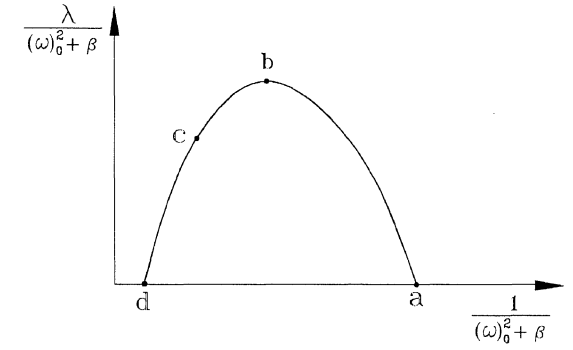

b) Transformed

Fig. 5 Bieigenvalue curve of a damped system.

Transformation of the Characteristic Curve

In Ref. 10, a procedure has been proposed for computing the critical load of an undamped nonconservative system. In this section, it will be demonstrated how the characteristic curve for a lightly damped structure can be transformed into one identical in form to that for the undamped structure. Let us start by rearranging Eq. (14):

$$\left(\frac{1+i\epsilon\omega}{\omega^2+\beta}[\bar{K}]-[\bar{M}]+\frac{\lambda}{\omega^2+\beta}[\bar{A}]\right)\{\hat{U}\}=\{0\} \tag{40}$$

where $\{\hat{U}\}$ denotes the eigenvector after transformation and

$$[\bar{A}]=[\bar{K}_g]-[\bar{K}_l] \tag{41a}$$

$$[\bar{K}]=[K_e]+\beta[M] \tag{41b}$$

Neglecting the higher-order term containing ϵ, Eq. (40) reduces to

$$\left(\frac{1}{\omega^2+\beta}[\bar{K}]-[\bar{M}]+\frac{\lambda}{\omega^2+\beta}[\bar{A}]\right)\{\hat{U}\}=\{0\} \tag{42}$$

The characteristic curve for the preceding equation is plotted in Fig. 5b. As can be seen, the slope at point b is zero:

$$\frac{\mathrm{d}[\lambda/(\omega^2+\beta)]}{\mathrm{d}[1/(\omega^2+\beta)]}=0 \tag{43}$$

from which the critical condition can be derived as

$$\beta+\omega^2=\lambda\frac{\mathrm{d}}{\mathrm{d}\lambda}(\omega^2) \tag{44}$$

This equation coincides with Eq. (39) for the original system.

Here, one observes that the characteristic curve abcd for the damped structure in Fig. 5a has been transformed into the curve dcba in Fig. 5b. A comparison of Eq. (44) with Eq. (39) indicates that point b in both Figs. 5a and 5b serves as the critical point. Because the system in Fig. 5b is identical in form to that for the undamped structure,[10] it will become unstable at point b where double roots occur. This same property should be carried over to point b of Fig. 5a for the lightly damped structure, where double roots are expected to occur as well.

Because the characteristic curve for the lightly damped system has been transformed into one identical to that for the undamped system, the critical load can be solved from the transformed system using the procedure described in Ref. 10 for undamped systems. One key feature of this procedure has been the adoption of a fourth-order hyperbolic curve, referred to as the bieigenvalue curve, for approximating the load-frequency relation of the system considered. Such a curve can be uniquely determined once the first and second derivatives of the frequency with respect to the load parameter are calculated, based on the eigensolutions obtained for the first few modes. After the bieigenvalue curve is established, the critical load can be calculated by setting its first derivative equal to zero. Theoretically, the accuracy of the critical load can be iteratively improved through adjustment of the bieigenvalue curve to make it more fitting, based on the eigensolutions obtained for higher load levels. In practice, it can be demonstrated that even for the case with no iteration (i.e., based on the free vibration results), solution of rather good accuracy can still be obtained.

Numerical Examples

The damping matrix in Eq. (13) can be nondimensionalized:

$$[C]=(\zeta/\omega_0)\left(\omega_0^2[M]+\beta[K_e]\right) \tag{45}$$

where ω_0 is the fundamental frequency of the structure with zero damping in free vibration, ζ the (gross) damping ratio, and β the external damping ratio. All of the examples to be studied have been solved in Ref. 10 assuming zero damping. In this study, each member is modeled by 10 beam elements.

Beam Subjected to Transverse Follower Load

As shown in Fig. 6, a beam subjected to a transverse follower load P at end B is restrained against translations along three axes and rotation about the x axis at end A and against rotations about the y and z axes at end B. This beam can be conceived as half of a simple beam subjected to a load at the midpoint. The following data are assumed: length $L=270$ cm, Young's modulus $E=21\times10^5$ kg/cm^2, shear modulus $G=7.8\times10^5$ kg/cm^2, depth $b=15.36$ cm, width $t=0.75$ cm, area $A=18$ cm^2, moment of inertia $I_y=0.54$ cm^4, torsional constant $J=2.16$ cm^4, radius of gyration squared $r^2=19.71$ cm^2, and specific weight $\gamma=7.5\times10^{-3}$ kg/cm^3.

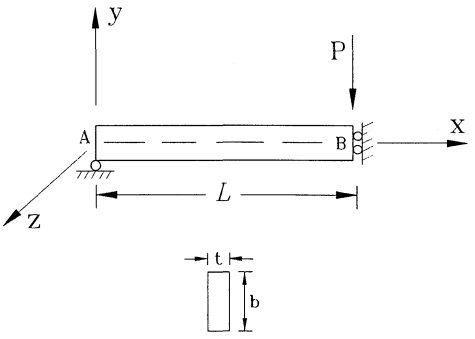

Fig. 6 Beam subjected to transverse follower load.

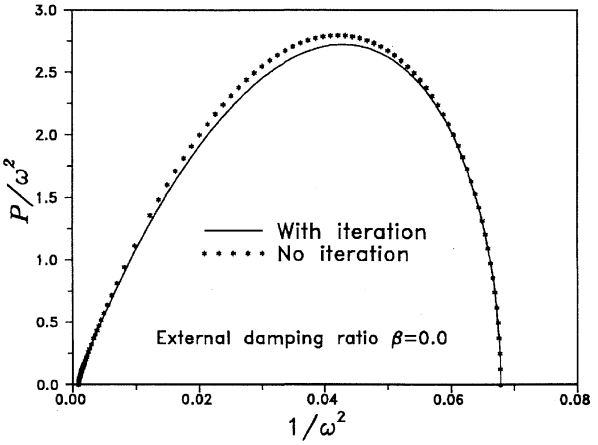

Fig. 7 Bieigenvalue curves for beam with transverse follower load.

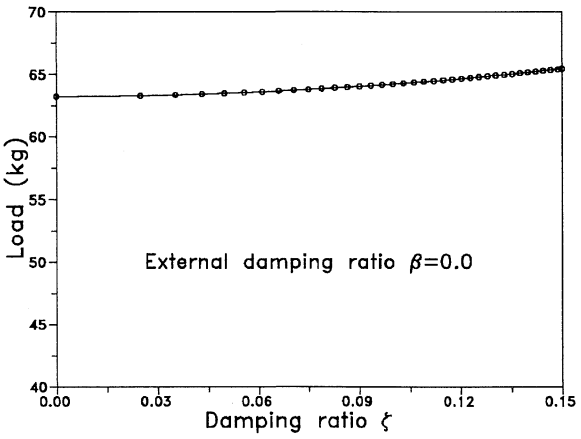

Fig. 8 Critical load vs damping ratio ζ.

For the case of small internal damping ($\beta=0$, $\zeta\to0$), the bieigenvalue curve established with no iteration, i.e., based merely on the free vibration results, and that based on iterative solutions of the complex eigenvalue problem at increasing load levels have been plotted in Fig. 7. As can be seen, the bieigenvalue curve established from the free vibration results is generally acceptable and on the conservative side.

For the case where only the effect of internal damping is concerned, i.e., with $\beta=0$, the critical load for dynamic instability has been plotted against the damping ratio ζ in Fig. 8. It can be seen

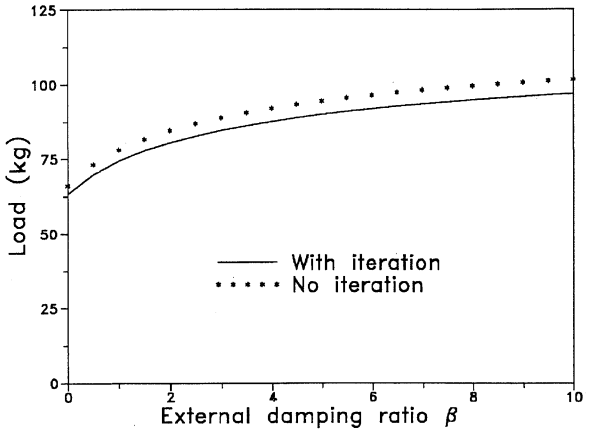

a) Critical load

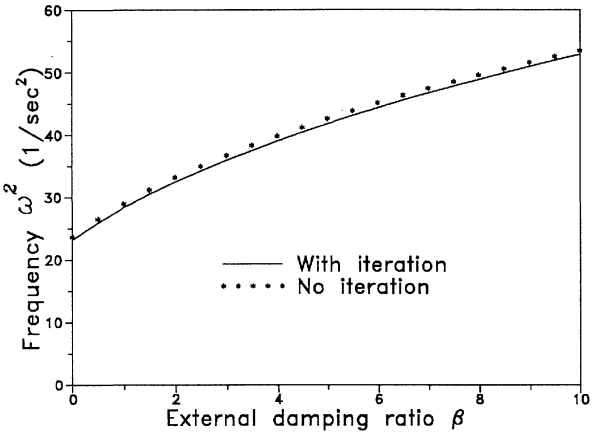

b) Frequency

Fig. 9 Beam with small internal damping.

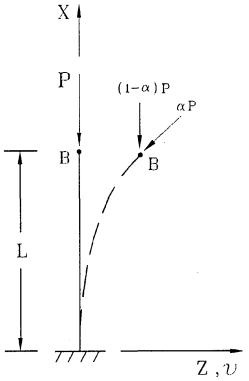

Fig. 10 Cantilever with nonconservative axial load.

that as the damping ratio ζ increases from 0 to 0.15, there is only a 3.5% increase on the critical load, implying that the critical load can be rather accurately predicted using a small damping ratio ζ. The critical load obtained from Fig. 8 for the case of small internal damping is 63.23 kg, which, when compared with the critical load of 110.5 kg for the undamped case, shows a drop of 40%. The discontinuity of the critical load at $\zeta = 0$ can be attributed primarily to the linearization involved in the perturbation procedure.

Based on the assumption of small damping, the critical load and frequency solved have been plotted against the external damping ratio β in Figs. 9a and 9b, respectively. It can be observed that the eigenvalues obtained with no iteration, i.e., based merely on the free vibration results, show an error not greater than 3.5% compared with those by iteration.

Cantilever with Nonconservative Axial Load

Figure 10 shows a cantilever subjected to an axial load P at the free end, of which αP indicates the nonconservative (follower)

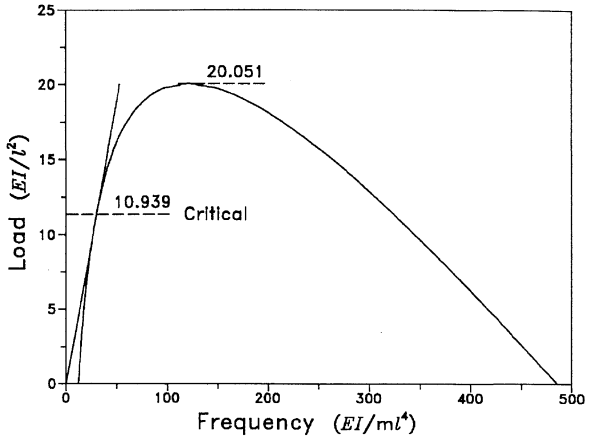

a) $\alpha = 1.0$

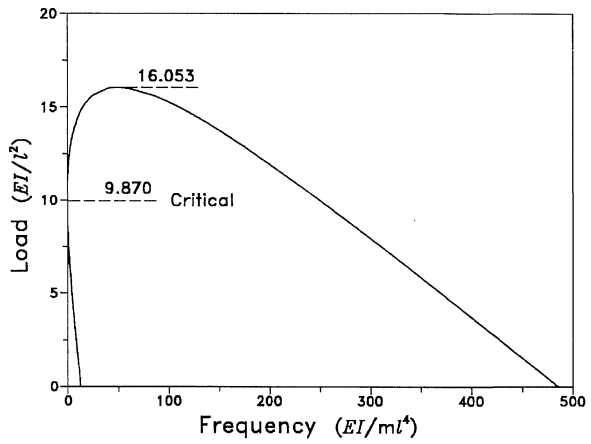

b) $\alpha = 0.5$

Fig. 11 Bieigenvalue curves for axially loaded cantilever.

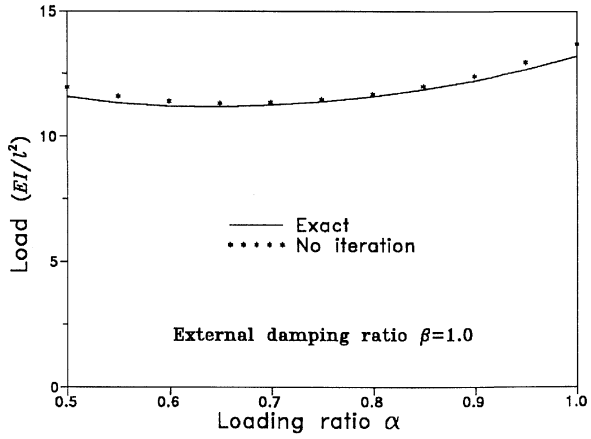

Fig. 12 Critical loads for axially loaded cantilever with $\zeta \rightarrow 0$ and $\beta = 1.0$.

part. For the case of small internal damping, i.e., with $\zeta \rightarrow 0$ and $\beta = 0$, the bieigenvalue curves established have been plotted in Figs. 11a and 11b for $\alpha = 1.0$ and 0.5, respectively. The critical loads obtained from Fig. 11 show a drop of 40% due to the existence of internal damping, compared with that for the undamped case.[10] For cantilevers with small damping ($\zeta \rightarrow 0$) and $\beta = 1.0$, the critical loads obtained from the bieigenvalue curves, either with or without iteration, have been plotted against the loading ratio α in Fig. 12. For $\alpha = 1.0$, the effect of internal and external damping on the critical load can be evaluated from Figs. 13a and 13b, respectively. As can be seen, a much larger increase on the critical load can be achieved through increase of the external damping, rather than the

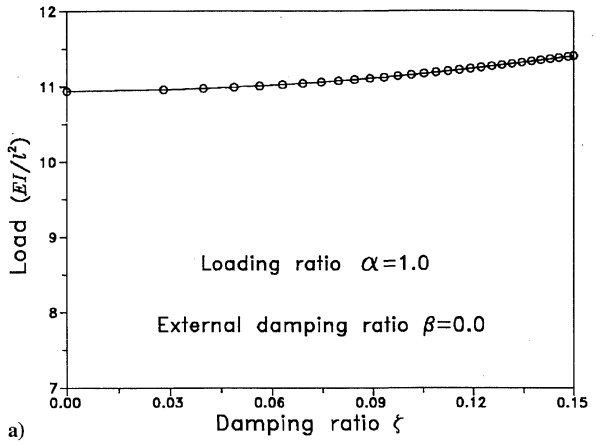

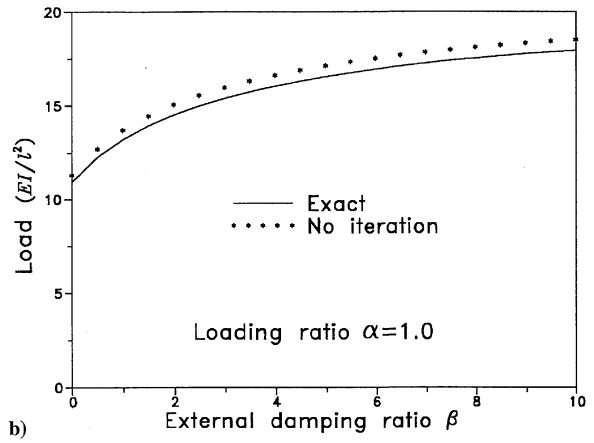

Fig. 13 Critical loads vs damping ratio and external damping ratio.

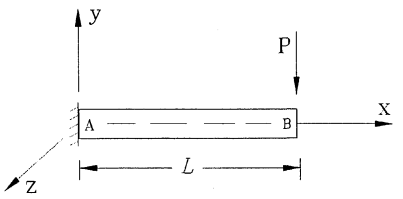

Fig. 14 Cantilever subjected to transverse follower load.

internal damping. For all of the cases where analytical solutions are available, it is observed that very good agreement has been made between the present results and the analytical ones.[14] Because all of the solutions obtained by the present approach with no iteration have been based merely on the eigensolution for the free vibration case, which does not rely on complex eigenvalue solvers, the superiority of the present approach to the other numerical approaches can be assured.

Cantilever Subject to Transverse Follower Load

The cantilever shown in Fig. 14 is subjected to a transverse follower load P at the free end. The same material and cross-sectional properties as those for the first example are adopted. For the case of small internal damping ($\zeta \to 0$, $\beta = 0$), the bieigenvalue curve established based on the eigensolution of the free vibration case has been compared with the one iteratively obtained in Fig. 15. It can be seen that even based merely on the free vibration results, the bieigenvalue established shows a rather high degree of accuracy.

The effect of internal damping ratio (i.e., with $\beta = 0$) can be appreciated from Fig. 16a. As the damping ratio ζ increases from 0 to 0.15, there is an increase of only 3% on the critical load. On the other hand, the critical load obtained for the present case with small internal damping is 67.8 kg, which is 40% less than that of the

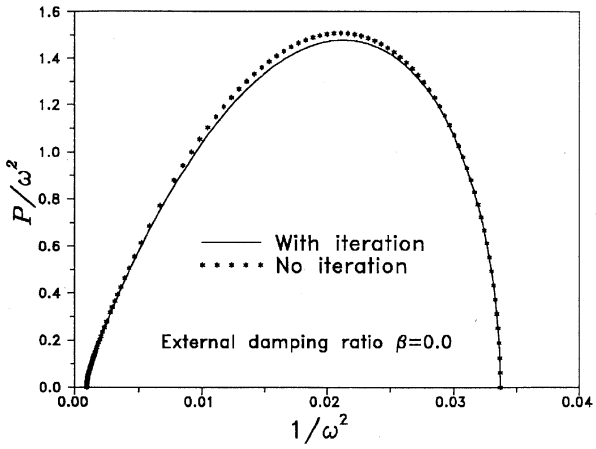

Fig. 15 Bieigenvalue curves for cantilever under transverse follower load.

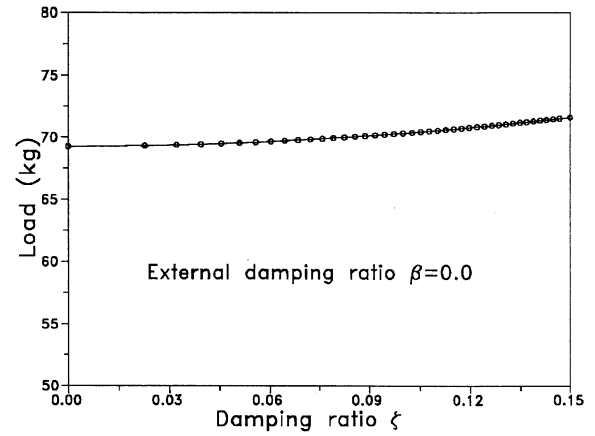

a) Internal

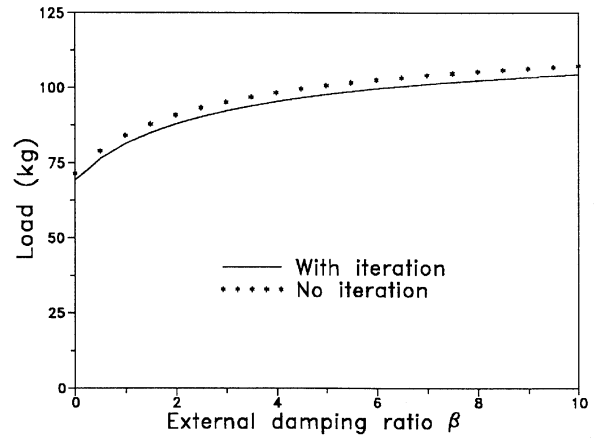

b) External

Fig. 16 Effects of damping on critical loads.

undamped case.[10] Assuming the damping ratio to be small, $\zeta \to 0$, the effect of external damping can be observed from Fig. 16b. Note that the critical loads obtained with and without iteration differ only by 3%.

Concluding Remarks

By the method of perturbation, the characteristic equation for a lightly damped linear nonconservative system can be transformed into a form identical to that for the undamped system. Using the bieigenvalue curve proposed in Ref. 10, rather accurate critical load can be computed for the system, even based on the free vibration results, which does not rely on complex solvers. Whenever iterations

are performed, generally three iterations are required to achieve convergent solutions. Compared with other existing methods, the present method's efficiency is considered superior. Other conclusions to be made include the following. 1) The existence of internal damping can reduce as much as 40% of the critical load of an undamped nonconservative system. 2) For the case of small internal damping, the critical loads can be marginally increased through increase of internal damping ratio. 3) The critical load of a nonconservative system can be significantly increased through use of larger external damping.

Acknowledgments

This study has been sponsored, in part, by Republic of China National Science Council Grant NSC80-0410-E002-18 and presented at the 19th International Congress of Theoretical and Applied Mechanics, Kyoto, Japan, Aug. 25–31, 1996.

References

[1]Bolotin, V. V., *Nonconservative Problems of the Theory of Elastic Stability* (Moscow), English translation, Pergamon, New York, 1963.

[2]Hermann, G., and Jong, I. C., "On the Destabilizing Effect of Damping in Nonconservative Elastic Systems," *Journal of Applied Mechanics*, Vol. 32, No. 3, 1965, pp. 592–597.

[3]Leipholz, H. H. E., *Stability of Elastic Systems*, Sijthoff and Nordhoff, Alphen aan den Rijn, The Netherlands, 1980.

[4]Ziegler, H., *Principles of Structural Stability*, 2nd ed., Birhäuser, Stuttgart, Germany, 1977.

[5]Barsoum, R. S., "Finite Element Method Applied to Problem of Instability of a Nonconservative System," *International Journal for Numerical Methods in Engineering*, Vol. 3, 1971, pp. 63–87.

[6]Mote, C. D., "Nonconservative Stability by Finite Element Method," *Journal of Engineering Mechanics*, Vol. 97, No. 2, 1971, pp. 645–656.

[7]Kounadis, A. N., "On the Failure of Static Stability Analyses of Nonconservative Systems in Regions of Divergence Instability," *International Journal of Solids and Structures*, Vol. 31, No. 15, 1994, pp. 2099–2120.

[8]Bolotin, V. V., Petrovsky, A. V., and Grishko, A. A., "Secondary Bifurcations and Global Instability of an Aeroelastic Non-Linear System in the Divergence Domain," *Journal of Sound and Vibration*, Vol. 191, No. 3, 1996, pp. 431–451.

[9]Chen, L. W., and Ku, D. M., "Stability of Nonconservative Systems Using Eigenvalue Sensitivity," *Journal of Engineering Mechanics*, Vol. 117, No. 5, 1991, pp. 974–985.

[10]Kuo, S. R., and Yang, Y. B., "Critical Load Analysis of Undamped Nonconservative Systems Using Bieigenvalue Curves," *AIAA Journal*, Vol. 32, No. 12, 1994, pp. 2462–2468.

[11]Paz, M., *Microcomputer-Aided Engineering Structural Dynamics*, Van Nostrand, New York, 1986, Chap. 11.

[12]Yang, Y. B., and Kuo, S. R., "Consistent Frame Buckling Analysis by Finite Element Method," *Journal of Structural Engineering*, Vol. 117, No. 4, 1991, pp. 1053–1069.

[13]Yang, Y. B., and Kuo, S. R., *Theory and Analysis of Nonlinear Framed Structures*, Prentice–Hall, Singapore, 1994, Chap. 6.

[14]Kuo, S. R., "Theory of Static and Dynamic Stability for Space Frames," Ph.D. Thesis, Dept. of Civil Engineering, National Taiwan Univ., Taipei, Taiwan, ROC, June 1991 (in Chinese).

G. A. Kardomateas
Associate Editor